Hindawi
Advances in Materials Science and Engineering
Volume 2023, Article ID 9821092, 1 page
https://doi.org/10.1155/2023/9821092

Retraction

Retracted: Postcare for Repairing Nerve and Tendon Injury Based on Biomimetic Nano-Parallel Material Composite Protein

Advances in Materials Science and Engineering

Received 26 December 2023; Accepted 26 December 2023; Published 29 December 2023

This article has been retracted by Hindawi, as publisher, following an investigation undertaken by the publisher [1]. This investigation has uncovered evidence of systematic manipulation of the publication and peer-review process. We cannot, therefore, vouch for the reliability or integrity of this article.

Please note that this notice is intended solely to alert readers that the peer-review process of this article has been compromised.

Wiley and Hindawi regret that the usual quality checks did not identify these issues before publication and have since put additional measures in place to safeguard research integrity.

We wish to credit our Research Integrity and Research Publishing teams and anonymous and named external researchers and research integrity experts for contributing to this investigation.

The corresponding author, as the representative of all authors, has been given the opportunity to register their agreement or disagreement to this retraction. We have kept a record of any response received.

References

[1] J. Fu, X. Tan, and Y. Tang, "Postcare for Repairing Nerve and Tendon Injury Based on Biomimetic Nano-Parallel Material Composite Protein," *Advances in Materials Science and Engineering*, vol. 2022, Article ID 1272673, 11 pages, 2022.

Hindawi
Advances in Materials Science and Engineering
Volume 2022, Article ID 1272673, 11 pages
https://doi.org/10.1155/2022/1272673

Research Article

Postcare for Repairing Nerve and Tendon Injury Based on Biomimetic Nano-Parallel Material Composite Protein

Junxia Fu, Xiaohong Tan, and Yan Tang

First People's Hospital of Chenzhou City (Hand and Foot Microsurgery), Chenzhou 423000, Hunan, China

Correspondence should be addressed to Yan Tang; tangyan@st.btbu.edu.cn

Received 11 May 2022; Revised 2 June 2022; Accepted 3 June 2022; Published 20 July 2022

Academic Editor: Haichang Zhang

Natural tendons are composed of ordered parallel arrangement of bundles of type I collagen fibers. It is responsible for transmitting the forces generated by the bones and muscles to move the body. Tendon injuries are common sports injuries, accounting for 50% of sports injuries. In adulthood, factors such as few tendon tissue cells and poor blood supply make it difficult to heal on their own after injury. Therefore, restoring the structure and function of native tendon tissue is still an unsolved problem. The purpose of this study is to study the use of biomimetic nano-parallel material composite proteins to induce the directional differentiation of stem cells to tendon lineages to promote muscle regeneration and repair. This study proposes to prepare composite protein nanomaterials by simulating the parallel arrangement of tendon collagen fibers. This can facilitate the directed differentiation of fibroblasts into tendon lineages. It can use the BP algorithm in the neural network algorithm to simulate the parallel arrangement of tendon collagen fibers, which is more efficient than other schemes. The experimental results in this study show that the rat cells are repaired after about 6 weeks. Tendon repair enters a remodeling phase with reduced cell numbers, collagen, and mucopolysaccharide synthesis. During this period, tendon repair gradually changes from the cellular level to the tissue level, and tenocyte metabolism remains high. Tenocytes and collagen fibers are aligned in the direction of stress. A higher proportion of collagen 1 synthesis occurs during this period. Collagen 1 accounts for 65% to 80% of the dry weight of the tendon, which plays the most important role in the mechanical properties of the tendon.

1. Introduction

At present, nanomaterials can be widely used in many fields because of their unique physical and chemical properties. In the field of clinical medicine, some biomedical nanomaterials are often introduced into blood tissue by intravenous injection, infiltration, dissolution, diffusion, etc. Tendon injury is one of the most common clinical symptoms. According to the American Board of Osteopathic Medicine, there are more than 32,000,000 cases of musculoskeletal injuries each year, of which tendon/ligament injuries account for about 45% because the integrity of tendon tissue depends on two factors: muscle healthy cells and extracellular matrix. The repair process after muscle bond injury is the process of cell proliferation, migration, and secretion of extracellular matrix. Therefore, how to regulate the rapid proliferation and migration of tenocytes and participate in the secretion of extracellular matrix is the decisive factor for tendon regeneration. Therefore, this study uses nano-parallel material composite protein to construct a biomimetic microenvironment, induces the directional differentiation of stem cells to tendon system, and promotes tendon regeneration and repair, which provides a new strategy for the treatment of tendon injury.

(1) First, artificial tendon repair has a long history. It is from the most primitive silk, collodion to later silicone rubber, Teflon rod, carbon fiber, small intestinal submucosa, etc. However, these materials have their limitations, such as poor biocompatibility, low degradation rate, and inability to simulate the micronano topology of natural tendon tissue, which results in unsatisfactory tendon regeneration. The biomimetic nano-parallel material composite protein is different from it in that it can induce the

directional differentiation of fibroblasts to the tendon system. (2) Second, the ideal tendon tissue replacement material should have the same micronano structure and physicochemical properties as the natural tendon. It has good biocompatibility and biodegradability, mechanical properties, and mechanical strength. It acts as a temporary extracellular matrix, providing a favorable microenvironment for growth, thereby promoting cell differentiation. (3) Finally, it simulates the parallel arrangement of tendon collagen fibers to prepare parallel ordered nano-parallel material composite proteins. This can induce the directional differentiation of fibroblasts to the tendon system, so as to achieve the effect of repairing the nerve tendon.

2. Related Work

Ulloa F believed that damage to the network can be repaired through a process of neurogenesis, which in turn can reestablish synapses between injured axons and postsynaptic terminals [1]. Utku et al. successfully prepared fibroin/hydroxyapatite scaffolds by dissolving fibroin and hydroxyapatite in phosphate buffer [2]. Ressler et al. learned from research that the nanocomposite structure of bone can be simulated by chitosan/hydroxyapatite (CS/HAp) composite scaffold [3]. Vurat et al. developed a novel osteogenic composite nanocoating for titanium surfaces. It provides an environment for promoting the adhesion of MSCs [4]. Ling et al. demonstrated a novel biomimetic strategy to assemble layered materials from biological nanobuilding blocks [5]. Zhuang et al. reported a hybrid natural-synthetic nanodelivery platform. This platform combines the biocompatibility of natural red blood cell membranes with the oxygen-carrying capacity of perfluorocarbons [6]. Liu et al. combined synthetic polymer scaffolds with inorganic bioactive factors. It is widely used to promote the biological activity and osteoconductivity of bone tissue [7]. However, the practicality of these studies is not strong enough.

3. A Method for Constructing Nanomaterial Composite Proteins Using Neural Networks

3.1. Artificial Neural Network Model

Definition 1. A neural network is a computational model. It consists of a large number of interconnected nodes. Each node represents a specific output function, which is called the excitation function. Each connection between two nodes represents a weighted value for the signal passing through the connection, which is called a weight. This is equivalent to the memory of an artificial neural network. The network itself is usually an approximation of a certain algorithm or function in nature, and it may also be an expression of a logic strategy.

It takes u as the internal state of the neurons that make up the neural network, S_I as the threshold, X as the input signal, and θ_i as the connection weight. Y represents the external input signal (in some cases it can control the neuron u, keeping it in a certain state). As shown in Figure 1, the above assumptions can be described as follows:

$$\begin{aligned} \sigma_i &\approx \sum x_i w_{ij} + s_i - \theta_i, \\ u_i &= f(\sigma_i), y_{i=} V(u_i) = g(\sigma_i). \end{aligned} \tag{1}$$

3.2. Types of Neuron State Transition Functions. When a neuron has no internal state, it can make $y_i = u_i$ and $h = f_0$. Commonly used neuron state transition functions are as follows:

Step function is as follows:

$$y = f(o) = \begin{cases} 1 & \sigma \geq 0, \\ 0 & \sigma < 0. \end{cases} \tag{2}$$

Quasilinear function is as follows:

$$y = f(o) = \begin{cases} 1 & \sigma \geq \alpha, \\ \sigma & 0 < \sigma < \alpha, \\ \sigma & \sigma < 0. \end{cases} \tag{3}$$

Sigmoid function is as follows:

$$y = f(o) = \frac{1}{1 + e^{-x}}. \tag{4}$$

Hyperbolic tangent function is as follows:

$$f(\sigma) = \frac{1}{2}\left(1 + th\left(\frac{\sigma \mathrm{i}}{\sigma 0}\right)\right). \tag{5}$$

Several forms of the above activation function represent that the activation function performs nonlinear of the difference between the weight of the input signal and the threshold. The mapping result y is used as the output signal, which is generally limited to a certain range ((0, 1) or (–1, 1)).

3.3. Introduction to BP Algorithm. The BP algorithm is composed of two processes, the forward propagation of the signal and the backpropagation of the error. Because the training of the multilayer feedforward network often adopts the error backpropagation algorithm, people often refer to the multilayer feedforward network directly as the BP network.

3.3.1. BP Neural Network Structure. In the process of outputting results, if the results of the output layer do not meet our expectations, the network enters the backpropagation stage. The network can in turn adjust the weights and thresholds of the network according to the prediction error. This makes the predicted output of the BP neural network continuously approach the expected output [8]. In this study, it uses the model construction and algorithm of neural network to simulate the parallel arrangement of tendon collagen fibers. It can also model the structure of biomimetic nano-parallel material composite proteins. Figure 2 shows the topology of the BP neural network.

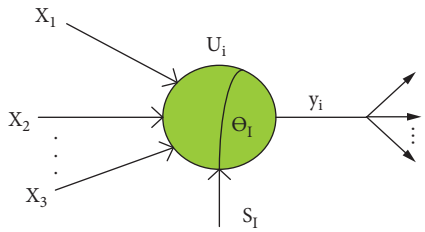

Figure 1: Neuron model.

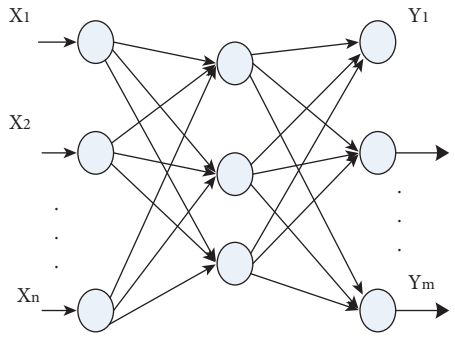

Figure 2: Topological structure of BP neural network.

3.3.2. Determined and Selected Network Structure. In order to determine and select the input layer, output layer, hidden layer, and the number of nodes in each hidden layer, it is necessary to determine the transfer function and error function of the number of nodes and also need to select each adjustable parameter value. The structure of a three-layer forward neural network based on the BP algorithm is shown in Figure 3.

The transfer function of the neuron is chosen as the sigmoid function:

$$f(x) = \frac{1}{1+\exp(-2x/u_0)},$$
$$f'(x) = \frac{2}{u_0} f(x)(1-f(x)). \tag{6}$$

The error function is a quadratic error function:

$$E = \frac{1}{2}\sum_{P=1}^{M}(T_P - Y_P)^2. \tag{7}$$

3.3.3. Initialization. It sets the number of learning $t=0$. It assigns small random numbers such as $w_2(t) \in [-1,1]$, $w_g(t) \in [-1,1]$ and $o_2(t) \in [-1,1]$ to the network weights and thresholds. It inputs a learning sample, where $K \in \{1,2\ldots,N\}$, N is the number of samples, and $T \in R$. It uses this to calculate the output value of each node in the hidden layer:

$$Y = f\left(\sum_{i=1}^{n} W_{ij}Y_j^1 - \theta j\right) = f\left(\sum_{i=1}^{n} W_{ij}X_{Ki} - \theta_j\right) \quad j \in \{1,2,\ldots,n_t\}. \tag{8}$$

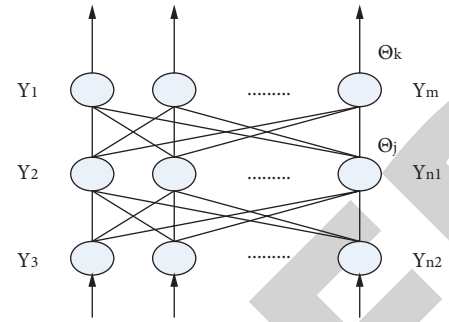

Figure 3: A three-layer feedforward neural network.

It computes the output of the output layer node:

$$Y_k^3 = f\left(\sum_{j=1}^{p} W_{jk}Y_j^2 - \theta_k\right) \quad k \in \{1,2,\ldots,\mathrm{m}\}. \tag{9}$$

3.3.4. Reverse Error Correction Calculation. The calculation of the connection weight correction between the output layer node and the hidden layer node is as follows:

$$\delta_k = \left(T_k - Y_k^3\right)Y_k^3\left(1-Y_k^3\right). \tag{10}$$

Calculation of connection weight correction between hidden layer nodes and output layer nodes is as follows:

$$\delta_j = Y_j^2\left(1-Y_j^2\right)\sum_{k=1}^{m}\delta_k W_{jk},$$
$$W_{ij}(t+1) = W_{ij}(t) + \alpha\delta_j Y_i^1 \quad . \tag{11}$$
$$\theta_j(t+1) = \theta_j(t) + \alpha * \delta_j.$$

Under certain conditions, feedforward neural networks can approximate any continuous function. Then, we can use it for supervised learning. It uses the principle of minimum error to train the feedforward neural network and finally makes it have the ability of self-adaptive solving. In addition, we also need to consider how to adjust the weights and determine the parameters of the network itself [9]. Due to the addition of the hidden layer, the neural network is complicated and the learning difficulty is increased. The emergence of the backpropagation algorithm, namely, the BP algorithm, overcomes this difficulty. The letter diagram of the BP network is shown in Figure 4:

As can be seen from the figure, in the BP network, there are two kinds of signal flow, one is the working signal and the other is the error signal. The working signal refers to the forward propagation of the input signal after entering the BP network from the input end. It is calculated layer by layer by computing units, and finally outputs the actual output signal at the output [10]. The error signal refers to the comparison of the actual output signal of the network with the expected output. The error signal it produces is propagated back from the output and calculated, and finally, the network parameters are modified.

It is set in the nth iteration, the output signal of the jth neuron of the output layer is $y_j(n)$, and then the error signal of the unit is provided by the following equation:

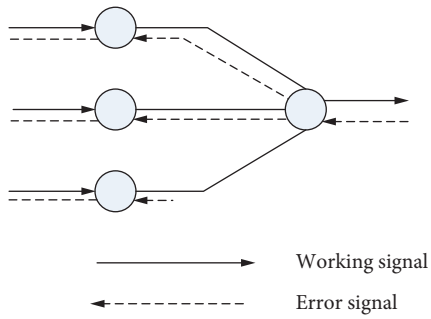

Figure 4: Signal diagram of BP network.

$$e_j(n) = d_j(n) - y_j(n). \tag{12}$$

It sets the average error of the neuron to $1/2e_j^2(n)$, and then the total squared error instantaneous value is calculated as follows:

$$\varepsilon(n) = \frac{1}{2}\sum_{jem} e_j^2(n), \tag{13}$$

m represents the number of neurons in the output layer.

It assumes that there are a total of N groups of training samples, and then the mean of the average error is calculated a follows:

$$\varepsilon_{AV} = \frac{1}{N}\sum_{n=1}^{N}\varepsilon(n) = \frac{1}{2N}\sum_{n=1}^{N}\sum e_j^2(n). \tag{14}$$

The BP algorithm is to continuously calculate the error value between the actual output signal and the expected output, then adjust the weight according to the error value, and finally make the objective function E_v reach the minimum value [11]. In the learning process, the adjustment of the weights can adopt the gradient information adjustment method. It can be adjusted according to formula (15). It sets p_{ij} as the connection weight of neuron i to neuron j, and then

$$\Delta p_{ji} = -\eta\delta_j(n)y_i(n). \tag{15}$$

To sum up, the artificial neural network is a practical science and technology. It is an adaptive nonlinear dynamic system composed of a large number of neuron connections with a complex structure. It has the ability of associative memory, parallel processing, self-adaptation, and abstract generalization. It also has good performance in noise tolerance. However, if gradient information is used to adjust the learning rules of connection weights, then it is easy to cause defects such as complicated calculation, slow learning speed, and easy to fall into local extreme values.

4. Experimental Design of Repairing Nerve and Tendon Injury Using Nanomaterial Composite Protein

4.1. Repair of Tendon Tissue by Complex Proteins. However, many investigators have demonstrated that injured and overloaded tendons or tenocytes are capable of secreting inflammatory mediators. In addition, there is an inflammatory response in the tissue where the tendon ruptures, especially after surgical treatment. The inflammatory response at the injury site is an important process in tendon repair. In the process of inflammation, the inflammatory hyperemia and exudative response can kill the injury factors and regulate the surrounding tissues and cells to participate in the repair of the injury site. On the other hand, the damaging factors released by inflammation can directly or indirectly cause tissue and cell destruction. The increase of inflammatory mediators is the main cause of pain. The excessive inflammatory response can cause tendinopathy, promote tendon tissue hyperplasia, and seriously affect the recovery of tendon function [12].

This research will work from the following aspects:

4.1.1. Primary Isolation, Culture, and Identification of Rat Tenocytes. It adopts the tissue block adherent culture method to separate and culture rat tenocytes. It is identified by observing cell morphology and detecting the expression of relatively specific marker molecules in the tendon.

4.1.2. The Effect of MGF-C25E on the Motility of Rat Tenocytes and Its Molecular Mechanism. It uses the scratch method and transwell method to detect the effect of MGF-C25E on tenocyte migration and invasion. It optimizes the optimal concentration of MGF-C25E to promote tenocyte migration and invasion. It further determined the mechanism of MGF-C25E in promoting tenocyte migration and invasion by techniques such as immunofluorescence staining, Western blot, and gelatin zymography.

4.1.3. The Role of Nuclear Mechanical Properties in MGF-C25E Promoting Tenocyte Migration. It determined the effect of MGF-C25E on nuclear stiffness by mechanical measurement of isolated and extracted nuclei by atomic force microscopy (AFM). It further determined the role and mechanism of nuclear mechanical properties affected by MGF-C25E in cell migration by PCR, Western blot, and immunofluorescence staining.

4.1.4. The Effect of MGF-C25E on Injured Tenocytes. It uses a cell mechanical loading device or tumor necrosis factor-alpha (TNF-α) to build a rat tenocyte injury model. It examines the effect of MGF-C25E on the repair of injured tendon at the cellular level.

4.1.5. Effects of MGF-C25E on the Repair of Injured Achilles Tendon in Rats. It uses rats as experimental animals to establish a rat Achilles tendon injury model. It evaluates the repair effect of MGF-C25E as a whole by comparing the functional index of injured tendon and normal tendon. It uses H&E staining and Masson's trichrome staining for histological evaluation of repaired tendons. It utilizes the Instron universal testing machine to detect the force-displacement curve of the repaired tendon. It analyzes biomechanical parameters such as ultimate displacement, ultimate stress, and hardness after repair of injured tendon

tissue. It evaluates the biomechanical properties of repaired tendons. The technical route is shown in Figure 5.

4.2. The Effect of MGF-C25E on Injured Tenocytes. The vitro tenocyte injury model is to intervene cells in an artificially simulated experimental environment and is mainly used to study the pathogenesis and repair mechanism of tendon. Clinical overuse of tendons is the main cause of tendon rupture and tendinopathy. The main method currently used in tendinopathy research is the mechanical stretching model [13]. Studies have shown that cyclic mechanical stretching can induce tenocytes to secrete a large number of inflammatory mediators, such as PGE, COX-1, and COX-2. In addition, overloading can lead to disordered fiber bundle arrangement and failure of biomechanical properties. The synthesis and degradation of collagen fibers can be used as important indicators of tendon injury. On the other hand, the action of certain cytokines can also trigger tendinopathy, such as tumor necrosis factor-alpha (TNF-α).

In this section, a rat tenocyte injury model was constructed by mechanical stretching and exogenous TNF-α. It uses qRT-PCR to detect rat tenocyte inflammatory index factors COX-2 and PGE, as well as collagen I and collagen III mRNA expression. It further examines the effect of MGF-C25E on injured tenocytes. The development of this part of the research work will provide a theoretical basis for MGF to participate in the repair of injured tendons.

4.2.1. Mechanical Stretching. The tensile loading device consists of a tensile unit, a control unit, and a silica gel culture chamber. The tensile deformation and frequency can be adjusted by the control unit [14].

The sterilization of the tensile loading device involves the following steps:

(1) *Sterilization of the Tensile Unit.* Before carrying out the loading experiment, it put the tensile unit of the tensile loading device into an ultraclean bench, wipe the entire device with a 75% alcohol cotton ball, and irradiate it with UV overnight.

(2) *Chamber Cleaning and Sterilization.* Since the chamber is a device that is used repeatedly, the chamber must be cleaned and sterilized after each use [15, 16]. First, it was ultrasonically cleaned with detergent-containing tap water for 15 min, and after the washing liquid was removed, it was ultrasonically cleaned with double-distilled water for 3 times for 15 min each time. Then it was soaked in triple-distilled water for 1 h, and finally was placed on the ultra-clean workbench for UV irradiation overnight, and was placed under sterile conditions for later use.

(3) *Cell Loading.* The effect of mechanical stimulation on tenocytes can be observed by cyclic uniaxial stretching of tenocytes using a cell-stretching device [17]. When the strain exceeds 8%, collagen fibers are prone to rupture and tendons are prone to damage. Studies have also shown that tenocytes can increase a tenocyte inflammatory response under mechanical loading of 12% deformation [18, 19]. In this study, a uniaxial mechanical stretching device was used to construct a rat tenocyte injury model under the conditions of 10% deformation and 1 Hz loading.

The primer sequences of rat collagen I, collagen III, COX-2, PGE2, and GAPDH are found from the literature and aligned in Pubmed. The five pairs of primer sequences that meet the requirements of qRT-PCR are listed in Table 1.

4.3. Construction of Rat Tenocyte Injury Model by Mechanical Stretching. After 10% deformation and 1 Hz mechanical loading for 24 h, qRT-PCR was used to detect the mRNA expressions of important tenocyte secreted factors collagen I and collagen III, as well as inflammatory index factors COX-2 and PGE. Mechanical loading at 1 Hz for 24 h significantly decreased the mRNA expressions of collagen I and collagen III in rat tenocytes ($p < 0.001$). It had no significant effect on the expression of inflammatory index factors COX-2 and PGE2 mRNA. It is suggested that mechanical loading may have no effect on the inflammatory response of tenocytes, but it can successfully induce the imbalance of collagen synthesis in tenocytes, which has a certain damage effect on tenocytes, as shown in Figure 6:

4.4. TNF-α to Build Rat Tenocyte Injury Model. In this study, 10 ng/mL TNF-α was used to induce the tenocyte inflammatory response. It can be seen that 10 ng/mL TNF-α could significantly reduce the mRNA expression of collagen I and collagen III in rat tenocytes ($p < 0.01$), and it had a significant promoting effect on the expression of COX-2 and PGE mRNA ($p < 0.01$). It is suggested that TNF-α can successfully induce the dysregulation of collagen synthesis in tenocytes and promote the inflammatory response of tenocytes in rats.

This study compares the tenocyte injury models constructed by the two methods, and it can be found that both methods make the collagen synthesis of tenocytes deregulated. It has a certain damaging effect on tenocytes, and TNF-α can also promote the expression of inflammatory factors in tenocytes, so that the cells have a certain inflammatory response. Since the mechanical loading process is complicated, we will use TNF-α to construct a rat tenocyte injury model in the subsequent experiments. The experimental results are shown in Figure 7.

4.5. Effect of MGF-C25E on Injured Tenocytes. To determine the effect of MGF on injured tenocytes, we examined the effect of MGF-C25E on TNF-α-altered collagen I, collagen III, COX-2, PGE, and mRNA expression. MGF-C25E (10–100 ng/mL) had no significant effect on TNF-α-reducing collagen I and collagen III but could reduce TNF-α-promoted COX-2 and PGE. With the increase of MGF-C25E concentration, its downregulation effect on COX-2 and PGE was more obvious. Under the action of high concentration of MGF-C25E (100 ng/mL), the decrease of COX-2 was significantly different from that of TNF-α-treated group ($p < 0.05$). These experimental results suggest that MGF-

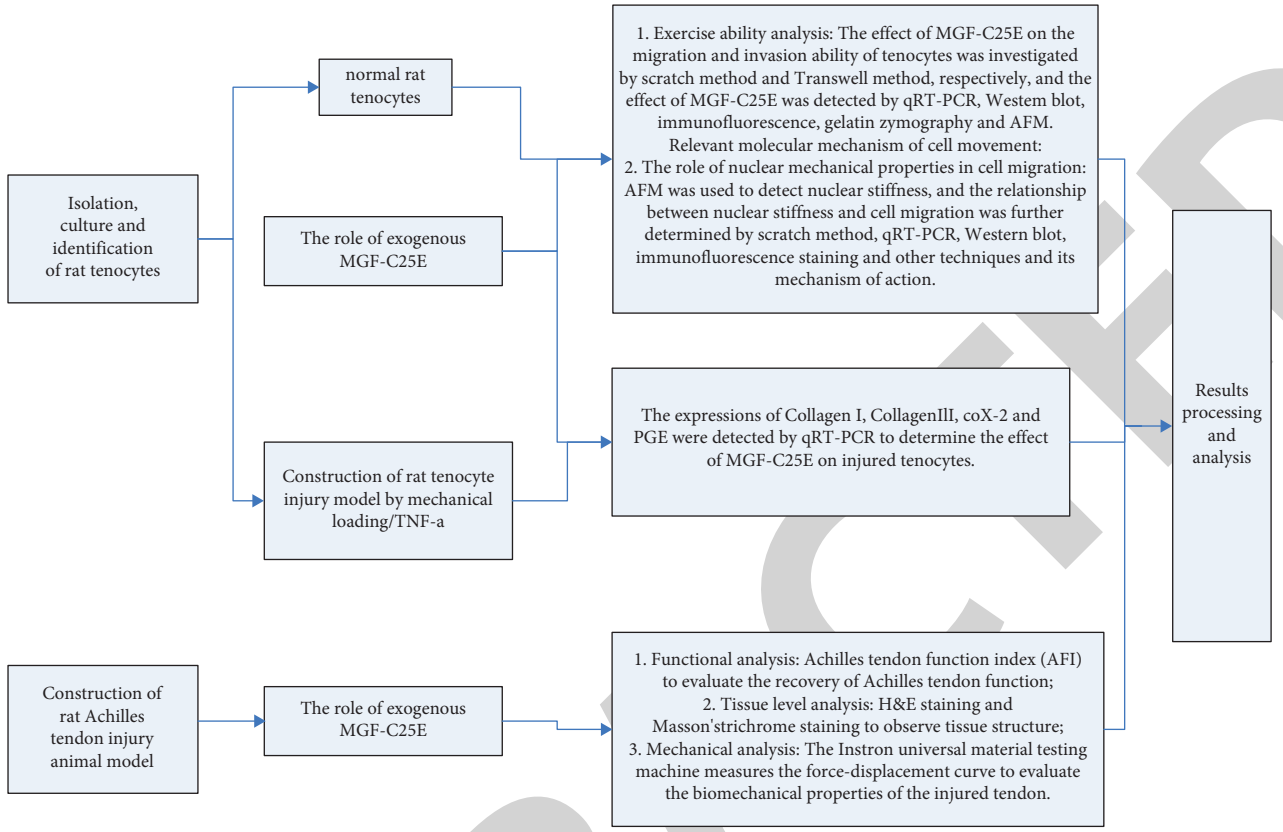

Figure 5: Technology roadmap.

Table 1: Sequence list of 5 pairs of primers.

name	Primer		Product length	Reference sequence
Collagen l	Sense Antisense	5′-GGAGAGAGTGCCAACTCCAG-3′ 5′-CTCGGCAGGTGTTCGGTA-3′	182 bp	NM_053304.1
Collagen III	Sense Antisense	51-TCCCAGAACATTACATACCACT-3 ′5′-GCTATTTCCTTCAGCCTTGA-3″	126 bp	NM_032085.1
Cox-2	Sense Antisense	5′-TGTATGCTACCATCTGGCTTCGG-3′ 5′-GTTTGGAACAGTCGCTCGTCATC-3′	94 bp	NM_017232.3
PGE	Sense antisense sense Antisense	5-CTCAAGACCTACCTGGTTTCA-3″ 5′-TTTCCGCCATACATCTGC-3″	161 bp	NM_001107832.1
GAPDH	Sense Antisense	5-AAGTTCAACGGCACAGTCAAGG-3′ 5′-CGCCAGTAGACTCCACGACATA-3	139 bp	NM_017008.4

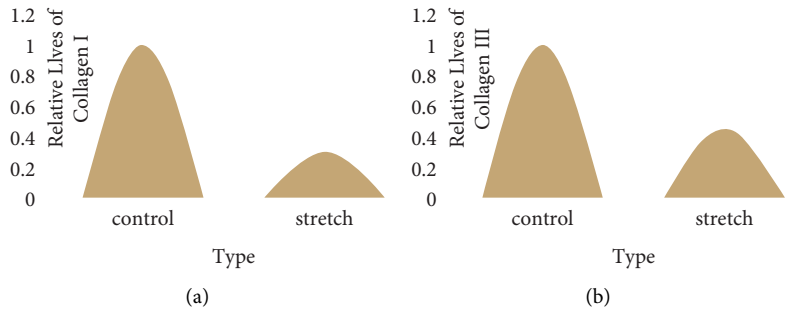

Figure 6: Effects of 10% strain and 1 Hz mechanical stretching for 24 h on the expression of tenocyte-related genes in rats. (a) Relative longevity of type I collagen. (b) Relative longevity of type III collagen.

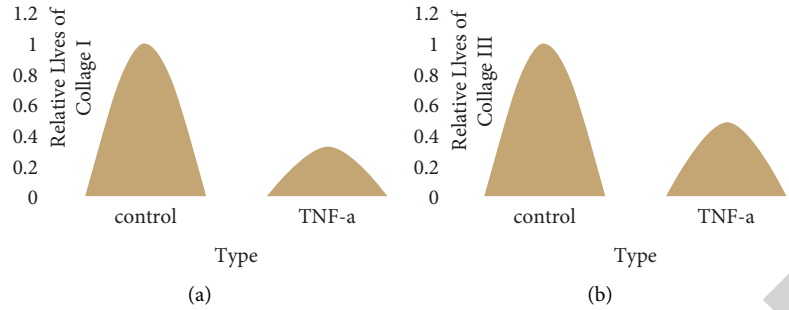

Figure 7: Effect of TNF-α (10 ng/mL) on the expression of tenocyte-related genes in rats. (a) Relative longevity of type I collagen. (b) Relative longevity of type III collagen.

C25E may have a certain anti-inflammatory effect on inflamed tenocytes. The experimental results are shown in Figure 8.

4.6. Vivo Repair Effect of MGF-C25E on Injured Achilles Tendon in Rats. The above research results show that MGF-C25E promotes the migration and invasion of rat tenocytes, and it has a certain inhibitory effect on the expression of inflammatory factors. Cell migration is an important link in the repair of tendon injuries [20]. Inflammation is the body's defense response to stimuli. Inflammation is often beneficial and is an automatic defense response of the body, but inflammation is also a major cause of pain, tissue necrosis, and lesions [21, 22]. Based on the previous research results, this section constructed a rat Achilles tendon injury model by surgical incision and suture. After exogenous injection of MGF-C25E, the effect of MGF-C25E on the repair of injured rat Achilles tendon was investigated in terms of functional recovery, mechanical properties, and tissue structure. In this study, the histological scoring system was used to score the experimental results by a single-blind method. The results are listed in Tables 2 and 3.

From Tables 2 and 3, it can be seen that the gait analysis was used to calculate the AFI value, and we tested the effect of MGF-C25E on the functional recovery of the injured Achilles tendon. Before the injury, the AFI value of the rats in each group was about −10, and the AFI value of each group decreased to about −70 after the injury (the first day after the operation). The lower the AFI value, the worse the Achilles tendon function. In the first 7 days after the operation, there was no significant change in the AFI value in each group, and the AFI value in each group gradually increased with the increase of repair time. Compared with the control group, the AFI value of MGF-C25E increased significantly. On the 21st day after the operation, the AFI value of the 1000 ng/mL MGF-C25E treatment group basically returned to a normal level. The above results show that MGF-C25E has a significant promoting effect on the functional recovery of injured Achilles tendon. The experimental results are shown in Figure 9.

4.7. Effects of MGF-C25E on Biomechanical Properties of Injured Rat Achilles Tendon. On the 21st postoperative day, tendon tissue was extracted to test the mechanical properties of the repaired Achilles tendon. The maximum rupture force of normal tendon was 56.5 ± 14.84 N, and the maximum rupture force after injury was 32.53 ± 3.29 N, which was significantly lower than that of normal tendon ($p < 0.01$). After MGF-C25E treatment, the maximum breaking force of the high-concentration MGF-C25E (1000 ng/mL) treatment group increased compared with the control group (injury + normal saline), but there was no significant change ($p > 0.05$). A high concentration of MGF-C25E (1000 ng/mL) significantly reduced the maximum displacement at tendon rupture ($p < 0.05$), which significantly increased the tissue stiffness at the rupture site. The experimental results are listed in Table 4.

4.8. Effect of MGF-C25E on the Tissue Structure of Injured Rat Achilles Tendon. On the 21st postoperative day, samples were extracted for the frozen section. The results of H&E staining showed that normal tendon tissue was rich in the extracellular matrix, with cells arranged in parallel, less in number, and uniform in the nucleus and cytoplasm. After an injury, the number of cells increased significantly, and the arrangement of cells became disordered. After MGF-C25E treatment, the high-concentration MGF-C25E (1000 ng/mL) treatment group increased the content of extracellular matrix and decreased the number of cells compared with the control group (injury + normal saline). The results of Masson's trichrome staining showed that the high-concentration MGF-C25E (1000 ng/mL) treatment group contained more abundant collagen fibers than the control group (6.5 b). Based on these experimental results, the histological scores showed that the high-concentration MGF-C25E (1000 ng/mL) treatment group (7.33 ± 0.58) had higher histological scores than the control group (3.67 ± 0.58) ($p < 0.01$, 6.5e). The experimental results are shown in Figure 10.

5. Postrepair Results

5.1. Effect of 10% Deformation and 1 Hz Mechanical Loading for 24 Hours on Inflammatory Factors in Rat Tenocytes. In this study, a cell tension loading device was used to construct a rat tenocyte injury model, and the mRNA expressions of collagen I, collagen III, and inflammatory index factors COX-2 and PGE were detected by qRT-PCR to

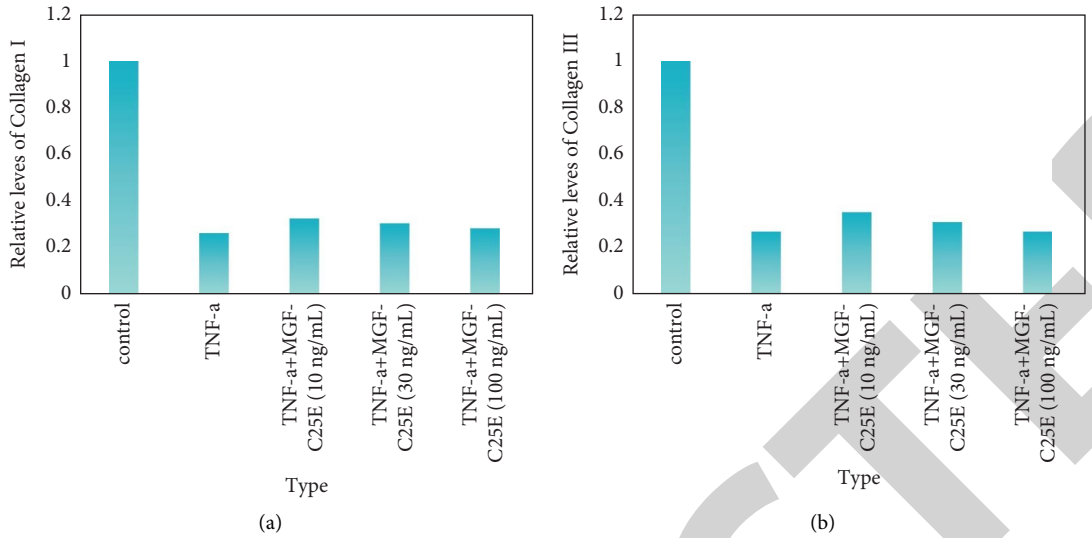

Figure 8: Effects of MGF-C25E on the expression of genes related to injured tenocytes. (a) Relative longevity of type I collagen. (b) Relative longevity of type III collagen.

determine whether the injury model was successfully constructed. The experimental results showed that 10% deformation and 1 Hz mechanical stretching for 24 h could significantly reduce the levels of collagen I and collagen III mRNA in rat tenocytes. It had no significant effect on COX-2 and PGE mRNA expressions.

5.2. Construction of Rat Tenocyte Injury Model with TNF-α. TNF-α is a widely recognized inflammation-promoting factor that can successfully induce a variety of cellular inflammatory responses. PGE is an important indicator of tendon inflammation and can cause tendon pain. COX-2 is an enzyme necessary for prostaglandin synthesis and is a key rate-limiting enzyme in the initial steps of prostaglandin synthesis. COX-2 can be induced by various damaging chemical, physical, and biological factors, then catalyzes the synthesis of prostaglandins, and participates in the inflammatory response. Since the mechanical stimulation simulated in vitro in this experiment could not induce the tenocyte inflammatory response, we will use TNF-α to construct a rat tenocyte injury model in the subsequent experiments. The establishment of rat tenocyte injury model by TNF-α can help us to investigate the effect of MGF-C25E on the repair of injured tendon at the cellular level.

5.3. Effect of MGF-C25E on Reducing TNF-α-Promoted COX-2 and PGE. The effects of MGF-C25E on TNF-α-promoted tenocytes COX-2 and PGE > mRNA expressions were detected by qRT-PCR. The experimental results showed that within the tested concentration range of MGF-C25E, with the increase of MGF-C25E concentration, TNF-α promoted tenocyte COX-2 and PGE, and mRNA expression was gradually downregulated. A large number of studies have proved that MGF can promote the repair of damaged tissue by increasing cell proliferation, migration, antiapoptosis, and other biological behaviors. But no studies have shown that MGF has anti-inflammatory effects. Inflammation is a common clinical-pathological process, in addition to tendons, it can also occur in various tissues and organs of the body. Anti-inflammatory drugs are used to treat the inflammatory response that occurs when tissue is damaged. It mainly includes two categories: one is steroidal anti-inflammatory drugs and the other is nonsteroidal anti-inflammatory drugs (NSAIDs). NSAIDs are a class of anti-inflammatory drugs that do not contain steroid structures. They all inhibit the final production of prostacyclin (PGI1), prostaglandin (PGE), and thromboxane A2 (TXA2) from arachidonic acid by inhibiting the activity of COX. Although this part of the work only examined the effect of MGF-C25E on TNF-α-induced COX-2 and PGE2 from the mRNA level, it also suggested that MGF may have the ability to reduce the inflammatory response of tenocytes. It may play an active role in the repair and regeneration of damaged tissue as an anti-inflammatory drug. However, more sophisticated assays are needed to determine the effect of MGF on tenocyte inflammatory responses. This will contribute to a more accurate and comprehensive understanding of the role and mode of action of MGF in injured tendon repair.

In our experiments, the Achilles tendon function recovered more rapidly in the high-concentration MGF-C25E-treated group than in the control group. This experimental result indicates that MGF-C25E has the effect of promoting the recovery of Achilles tendon function in rats. It can be seen from the above that MGF-C25E can reduce the TNF-α-induced increase in COX-2 and PGE mRNA expression, which suggests that MGF-C25E may have a certain anti-inflammatory effect. Inflammation is the first physiological response to tendon rupture. During this process, a large number of inflammatory cells migrate to the site of injury. It then secretes a large number of inflammatory regulators involved in the repair and regeneration of injured tendons, such as I-13, COX2, and PGE. PGE can cause vasodilation and trigger pain sensation. It can be used as an

Table 2: Morphological scoring system.

Parameter	Point
Loading/lameness	
Hind leg fully loaded	1
Hind leg not fully loaded	0
Connection tendon to SN/slidability	
Not conjoined, slidable	1
Adhesion, not fully slidable	0
Tendon rupture	
Nonexisting	1
Existing	0
Inflammation	
Nonexisting	1
Existing (oedema, swelling, and redness)	0
Tendon surface at the surgery area	
Intact, smooth	1
Uneven, harsh	0
Connection tendon paratendineum and fascia, slidability	
Not adnated, slidable	1
Adhesion, not slidable	0
Swelling/redness of tendon	
No swelling/no redness	2
Palpable swelling with no redness	1
Palpable swelling with redness	0
Neighboring tendon	
Unchanged	1
Changed (color, thickness, and surface)	0
Shape of tendon	
Normal	3
Slightly thickened	2
Moderately thickened	1
Intensely thickened	0
Color of tendon	
Bright white	1
Translucent, dull white, and rose	0
Single strains of gastrocnemius muscle tendon	
Normal conjoined	1
Adhesion, heavily adnated	0

Table 3: Organizational scoring system.

Parameter	Point
ECM organization of the tendon	1
Way, compact, and parallel arranged collagen fibers	0
In part compact, in part loose, or not orderly arranged	
Loosely composed and not orderly arranged ("granulation" tissue)	2
Cell-to-matrix ratio	1
Physiological	0
Locally increased cell density	
Increased cell density or decreased ECM content	1
Cell alignment	0
Uniaxial	
Areas of irregularly arranged cells (10–509%)	2
More than 50% of cells with no uniaxial alignment	1
Cell distribution	0
Homogeneous, physiological	
Focal areas of cleaved cell density (cell clustering)	2
Cell nucleus morphology	1
Predominantly elongated, heterochromatic cell nuclei	0
10–30% of the cells possess large, oval, euchromatic, or polymorphic heterochromatic nuclei	
Predominantly larger, oval, euchromatic, or polymorphic, heterochromatic nuclei	2
Organization of repair tissue of homogeneous tendon cells	1
Locally heterogeneous tissue composition	0
Whole tissue composition completely changed	
Configuration of cells	
Normal, only in the surgery area, and locally confined	1
Strong, change of whole tendon, and thickened	0
Degenerative changes in metaplasia	
Nonexisting	2
Moderate formation of oedema	1
Intense oedema with inclusion of fat, cell, and or fibers destruction, fibrin deposition, and gaps inflammation	0
No inflammatory cell in filtrates	3
Slight inflammatory cell infiltrates	2
Moderate inflammatory cell infiltrates	1
Intense inflammatory cell infiltrates	0

indicator factor for tendon inflammation. Pain affects Achilles tendon function and directly leads to changes in the gait of rats when they walk. Therefore, we speculate that MGF-C25E promotes the early functional recovery of injured rat Achilles tendon because MGF-C25E has a certain anti-inflammatory effect.

The restoration of tendon mechanical properties is the most important reference for tendon preinjury repair. After the effect of MGF-C25E, the maximum breaking force of the high-concentration MGF-C25E (1000 ng/mL treatment group increased compared with the control group (injury + normal saline), but there was no significant difference. However, a high concentration of MGF-C25E (1000 ng/mL) reduced the maximum displacement of tendon rupture, and the tissue stiffness was significantly enhanced compared with the control group ($p < 0.05$). The mechanical properties of tendons are mainly determined by the collagen structure. The repair of damaged tendons is a long process, and after a brief inflammatory phase, it enters a proliferative phase. It begins to synthesize collagen 3 during the proliferative phase and gradually reaches its peak. This period usually lasts a few weeks. After approximately 6 weeks, tendon repair enters a remodeling phase with reduced cell numbers, collagen, and mucopolysaccharide synthesis. During this period, tendon repair gradually changes from the cellular level to the tissue level, and tenocyte metabolism remains high. Tenocytes and collagen fibers align in the direction of stress, and a higher proportion of collagen 1 synthesis occurs during this period. Collagen 1 accounts for 65% to 80% of the dry weight of the tendon and plays the most important role in the mechanical properties of the tendon. Our samples were collected on the 21st postoperative day, shortly after tendon repair entered the proliferative phase. It is an early stage of tendon repair, and the synthesis of collagen at this stage is mainly based on collagen 3. The increased synthesis of collagen 3 may form some network-connected structures, so we speculate that MGF-C25E has no significant effect on the maximal rupture force of the repaired tendon. However, it significantly increases its tissue strength. This is because MGF-C25E promotes collagen 3 synthesis during the early repair. In addition, the effect of collagen fibers on the mechanical properties of tendons is also affected by collagen

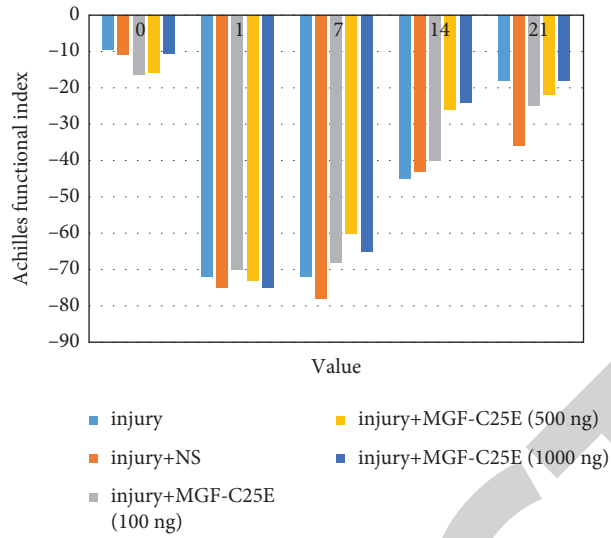

Figure 9: Effect of MGF-C25E on AFI of injured Achilles tendon.

Table 4: Mechanical measurement results.

Group normal	Failure load (N)	Displacement at break (mm)	Stiffness (N/mm)
Injury	56.514.84	1.15 ± 0.51	63.52 ± 43.46
Injury + NS	32.53 + 3.29	2.44 ± 0.51	13.64 ± 1.97
Injury + MGF-C25E (100 ng/mL)	32.77 ± 4.87	2.99 ± 0.43	10.97 ± 0.85
Injury + MGF-C25E (500 ng/mL)	28.87 ± 6.21	2.53 ± 0.89	12.8 ± 0.55
Injury + MGF-C25E (1000 ng/mL)	31.95 ± 7.97	2.68 ± 0.35	11.81 ± 1.94
Group normal	37.71 ± 3.87	1.79 ± 0.6	24.07 ± 10.08

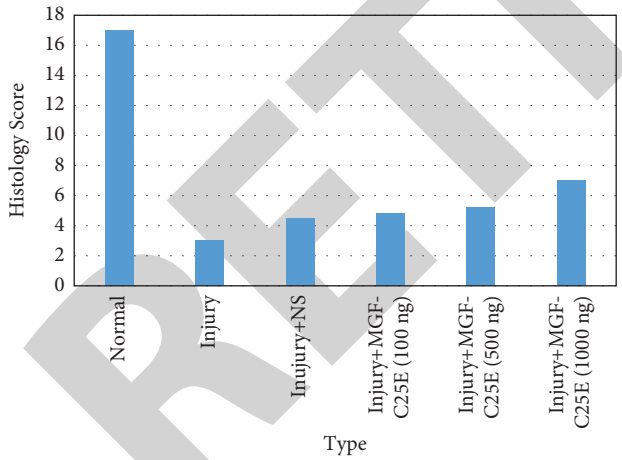

Figure 10: Histological analysis of repaired tendons.

arrangement, degree of collagen cross-linking, and amount of collagen secretion. In our histological examination, it can be found that the collagen content of normal tendons is very rich, the collagen bundles are neatly arranged, and the collagen content is significantly reduced after injury. Although the high-concentration MGF-C25E (1000 ng/mL > treatment group contained more abundant collagen fibers than the control group, but, its content is still very low compared to normal tendons. Therefore, MGF-C25E had no obvious effect on the maximum mechanical load that the repaired tendon could bear.

6. Conclusion

In conclusion, this study systematically studied the effect of biomimetic nano-parallel material composite protein on the migration and invasion of rat tenocytes. This study clarifies the signal transmission pathway from the cytoplasm to nucleus in the process of nanomaterial composite protein MGF-C25 affecting tenocyte motility. It provides an experimental basis for a deep understanding of the molecular mechanism of MGF-C25 affecting tenocyte movement. We constructed a tenocyte injury model and investigated the effect of MGF-C25 on the expression of inflammatory factors associated with injured tenocytes. It confirmed that MGF-C25 has the effect of reducing the expression of inflammatory factors in tenocytes. It suggests that MGF may promote the repair of injured tendon by reducing the inflammatory response of tenocytes. Finally, by constructing an animal model of rat Achilles tendon injury, this study systematically evaluated the effect of MGF-C25 on the repair of injured tendon from different perspectives such as functional recovery, biomechanical properties, and tissue structure. It proves that MGF-C25 has a certain promoting effect on the repair of injured tendon. It provides theoretical guidance and methodological reference for the clinical application of growth

factors such as MGF-C25 for better treatment of injured tendons.

Data Availability

No data were used to support this study.

Conflicts of Interest

The authors declare that they have no conflicts of interest.

References

[1] S. Araújo, F. Ulloa, T. Cotrufo, D. Ricolo, and E. Soriano, "SNARE complex in axonal guidance and neuroregeneration," *Neural Regeneration Research*, vol. 13, no. 3, p. 386, 2018.

[2] F. S. Utku, K. Basaran, and Y. Sunar, "Generation of silk Fibroin-Ca-P composite biomimetic bone replacement material using electrochemical deposition," *Istanbul University-Journal of Electrical and Electronics Engineering*, vol. 17, no. 2, pp. 3439–3443, 2017.

[3] A. Ressler, K. Zadro, H. Ivanković et al., "From bio-waste to bone substitute," *Chemical and Biochemical Engineering Quarterly*, vol. 34, no. 2, pp. 59–71, 2020.

[4] M. T. Vurat, A. E. Elçin, and Y. M. Elçin, "Osteogenic composite nanocoating based on nanohydroxyapatite, strontium ranelate and polycaprolactone for titanium implants," *Transactions of Nonferrous Metals Society of China*, vol. 28, no. 9, pp. 1763–1773, 2018.

[5] S. Ling, K. Jin, Z. Qin et al., "Combining in silico design and biomimetic assembly: a new approach for developing high-performance dynamic responsive bio-nanomaterials," *Advanced Materials*, vol. 30, no. 43, Article ID 1802306, 2018.

[6] J. Zhuang, M. Ying, K. Spiekermann et al., "Biomimetic nanoemulsions for oxygen delivery in vivo," *Advanced Materials*, vol. 30, no. 49, Article ID 1804693, 2018.

[7] S. Liu, Y. Zheng, R. Liu, and C. Tian, "Preparation and characterization of a novel polylactic acid/hydroxyapatite composite scaffold with biomimetic micro-nanofibrous porous structure," *Journal of Materials Science: Materials in Medicine*, vol. 31, no. 8, p. 74, 2020.

[8] T. Fan, J. Chen, and X. Liu, "Biomimetic preparation and characterization of Fe3O4-chitosan-collagen- nano hydroxyapatite in situ composite scaffold," *Fuhe Cailiao Xuebao/Acta Materiae Compositae Sinica*, vol. 34, no. 11, pp. 2593–2597, 2017.

[9] I. A. Neacsu, A. P. Serban, A. I. Nicoara, R. Trusca, V. L. Ene, and F. Iordache, "Biomimetic composite scaffold based on naturally derived biomaterials," *Polymers*, vol. 12, no. 5, p. 1161, 2020.

[10] A. Pitchaimani, T. Nguyen, and R. Marasini, "Biomimetic natural killer membrane camouflaged polymeric nanopartide for targeted bioimaging," *Advanced Functional Materials*, vol. 29, no. 4, pp. 1806817.1–1806817.11, 2019.

[11] C. Huang, S. Bhagia, N. Hao et al., "Biomimetic composite scaffold from an in situ hydroxyapatite coating on cellulose nanocrystals," *RSC Advances*, vol. 9, no. 10, pp. 5786–5793, 2019.

[12] R. A. Al-Shatti, G. H. Dashti, S. Philip, S. Michael, and M. V. Swain, "Size or hierarchical dependence of the elastic modulus of three ceramic-composite CAD/CAM materials," *Dental Materials*, vol. 35, no. 7, pp. 953–962, 2019.

[13] W. Zhang, H. Liu, W. Yang et al., "Hydroxyapatite/silk fibroin composite biomimetic scaffold for dental pulp repair," *Bioinspired, Biomimetic and Nanobiomaterials*, vol. 8, no. 4, pp. 231–238, 2019.

[14] A. Gupta, V. K. Patel, and C. Pandey, "Functional characterization of nano-porous silicate-polymer composite for bovine serum albumin immobilization," *Sensors International*, vol. 2, no. 5802, Article ID 100080, 2021.

[15] P. Dorishetty, R. Balu, S. S. Athukoralalage et al., "Tunable biomimetic hydrogels from silk fibroin and nanocellulose," *ACS Sustainable Chemistry & Engineering*, vol. 8, no. 6, pp. 2375–2389, 2020.

[16] T. Bao, M. M. Damtie, K. Wu et al., "Rectorite-supported nano-Fe3O4 composite materials as catalyst for P-chlorophenol degradation: preparation, characterization, and mechanism," *Applied Clay Science*, vol. 176, no. AUG, pp. 66–77, 2019.

[17] B. Szefler, "Nano-structures as materials in biosciences," *Journal of Molecular Structure*, vol. 1224, no. 6, Article ID 129186, 2021.

[18] M. Attar, S. M. Ahmadpour, S. S. Banisadr, A. Mohammadi, S. Z. Mirmoradi, and Z. Shirazi, "The effect of Al2O3 nano additions on failure of GFRP plate with two parallel pin loaded holes," *Journal of Mechanical Science and Technology*, vol. 33, no. 6, pp. 2769–2776, 2019.

[19] F. Nemavhola and R. Sigwadi, "Prediction of hyperelastic material properties of Nafion117 and nafion/ZrO2 nanocomposite membrane," *International Journal of Automotive and Mechanical Engineering*, vol. 16, no. 2, pp. 6524–6540, 2019.

[20] H. C. Robinson, A. Telser, and A. Dorfman, "Studies on biosynthesis of the linkage region of chondroitin sulfate-protein complex," *Proceedings of the National Academy of Sciences*, vol. 56, no. 6, pp. 1859–1866, 1966.

[21] M. Pelosse, H. Crocker, B. Gorda, P. Lemaire, J. Rauch, and I. Berger, "MultiBac: from protein complex structures to synthetic viral nanosystems," *BMC Biology*, vol. 15, no. 1, p. 99, 2017.

[22] A. Zeynali, T. S. Ghiasi, G. Riazi, and R. Ajeian, "Organic solar cell based on photosystem I pigment-protein complex, fabrication and optimization," *Organic Electronics*, vol. 51, no. DEC, pp. 341–348, 2017.